

Nucleon decay search in Super-Kamiokande

Makoto MIURA*

Kamioka observatory, ICRR, UTokyo

E-mail: miuram@icrr.u-tokyo.ac.jp

Nucleon decay search is one of keys for opening a door to Grand Unified Theories (GUTs). A favored proton decay mode by GUTs based on SU(5) symmetry is $p \rightarrow e^+ \pi^0$. On the other hand, SUSY moderated GUTs prefer $p \rightarrow \bar{\nu} K^+$. The Super-Kamiokande, a large water cherenkov detector, has been running more than 10 years and it is suitable for the nucleon decay search. In this paper, the latest results of nucleon decay searches in Super-Kamiokande are summarized.

*The 34th International Cosmic Ray Conference,
30 July- 6 August, 2015
The Hague, The Netherlands*

*Speaker.

1. INTRODUCTION

The standard model of elementary particle physics, based on $SU(3)$ for the strong interaction and the unification of $SU(2) \times U(1)$ for the electroweak interaction, has been successful in accounting for many experimental results. However, the standard model offers no guidance on the unification of the strong and electroweak interactions, and has several other open questions. Various attempts have been made to resolve the shortcomings by unifying the strong and electroweak interactions in a single larger gauge group, i.e. a Grand Unified Theory (GUT) [1]. GUTs are motivated by the apparent convergence of the running couplings of the strong, weak, and electromagnetic forces at a high energy scale ($10^{15} - 10^{16}$ GeV). Such large energy scales are out of the reach of accelerators but may be probed by virtual processes such as those that govern particle decay. A general feature of GUTs is the instability of nucleons by baryon number violating decay. Therefore nucleon decay experiments are direct experimental tests of the general idea of grand unification.

In GUTs, nucleon decay can proceed via exchange of a massive gauge boson between two quarks. The favored gauge-mediated decay mode in many GUTs is $p \rightarrow e^+ \pi^0$. GUT models incorporating supersymmetry [2] (SUSY-GUTs) raise the GUT scale [3], suppressing the decay rate of $p \rightarrow e^+ \pi^0$, thereby allowing compatibility with the experimental limit. However, SUSY-GUTs introduce dimension five operators that enable the mode $p \rightarrow \bar{\nu} K^+$ to have a high branching fraction and short partial lifetime [4].

This report describes results of search for major proton decay modes, $p \rightarrow e^+ \pi^0$, $p \rightarrow \mu^+ \pi^0$, and $p \rightarrow \bar{\nu} K^+$, by using 306 kiloton (kton) · year data of Super-Kamiokande.

2. SUPER-KAMIOKANDE

Super-Kamiokande (SK) [5] is a large water Cherenkov detector. It is an upright cylinder in shape, 39 m in diameter and 40 m in height, and it contains 50 kton of pure water. It lies about 1,000 m underneath the top of Mt. Ikenoyama (2,700 m water equivalent underground) to reduce cosmic ray background. The detector is optically separated into two regions: inner detector (ID) and outer detector (OD). Cherenkov light in the ID is detected by 20-inch PMTs [6] facing inward, evenly covering the cylindrical inner surface. Cherenkov light from penetrating particles, usually cosmic ray muons or exiting muons, is detected by 8-inch PMTs facing outward. Proton decays are rare phenomena and huge number of protons are needed for these search. In this meaning, water Cherenkov detector like SK is the best choice for proton decay search. In SK, fiducial volume is defined as a cylindrical volume with surfaces 2 meters inwards from the ID PMT plane. The fiducial mass is 22.5 ktons, corresponding to 7.5×10^{33} protons. Backgrounds for proton decay searches are caused by atmospheric ν interactions and they are well understood because SK is the most famous neutrino detector in the world. Table 1 summarizes the data sets used for the proton decay searches and total exposure of 306 kton · year is used for this paper.

3. $p \rightarrow e^+ \pi^0, \mu^+ \pi^0$

The proton decay mode in which a proton decays into a charged lepton and a neutral pion is regarded as a dominant mode in several GUT models. The neutral pion decays into two gammas

	Live days	kton·yr	Coverage
SK-I	1489.2	91.7	40%
SK-II	798.6	49.2	19%
SK-III	518.1	31.9	40%
SK-IV	2166.5	133.5	40%

Table 1: Summary of data sets that are used in this paper. Note that the photo coverage in SK-II was almost a half of the other periods. In SK-IV (current run), new electronics read out have been installed and it contributes for improving Michel electron tagging.

immediately thus all particles can be detectable by a water Cherenkov detector such as SK, that means, the proton mass and momentum can be reconstructed from detected Cherenkov rings. The following cuts are applied to data and MC; (A-1) the events are fully contained in the fiducial volume which is defined as inward from 2 meter from the detector wall (FCFV), (A-2) 2 or 3 rings and all rings should be e-like for $p \rightarrow e^+\pi^0$ and one ring should be μ -like for $p \rightarrow \mu^+\pi^0$, (A-3) there are no Michel electrons for $p \rightarrow e^+\pi^0$, one electron for $p \rightarrow \mu^+\pi^0$, (A-4) reconstructed π^0 mass should be $85 < M_{\pi^0} < 185 \text{ MeV}/c^2$ for 3 ring events, (A-5) reconstructed total mass should be $800 < M_{tot} < 1050 \text{ MeV}/c^2$ and reconstructed total momentum P_{tot} should be less than 250 MeV/c, and only for SK-IV, (A-6) there are no neutrons. Neutrons are captured by hydrogen and emit 2.2 MeV γ ray with about 200 μ sec lifetime. Upgraded electronics in SK-IV can keep all hit information and it enables to search for such delayed signal, as a result, neutron can be tagged by delayed γ . Backgrounds from atmospheric ν interactions often accompany with neutrons and cut (A-6) can reject almost 50% background. After proton decay in oxygen, on the other hand, remained nuclei emit γ dominantly at deexcitation, thus (A-6) reduces signal efficiency only by 5%.

In 306 kton·year data, no candidates observed for $p \rightarrow e^+\pi^0$ with 0.61 expected background. Figures 1 show M_{tot} vs P_{tot} after all cuts except (A-5) for signal MC, atmospheric ν background MC, and data. For $p \rightarrow \mu^+\pi^0$, two events observed while expected background is 0.87. Figures 2 show M_{tot} vs P_{tot} for signal MC, atmospheric ν background MC, and data. Both observed events have relatively higher P_{tot} and locate close to boundary of signal region defined by (A-5). Table 2 summarizes selection efficiencies estimated by signal MC, expected number of atmospheric ν backgrounds, and observed events for each periods. Lifetime limit with 90% C.L. is calculated by separating total momentum into two bins; $P_{tot} < 100 \text{ MeV}/c$ and $100 \leq P_{tot} < 250 \text{ MeV}/c$. As seen in Figure 1 and Figure 2, free protons, which don't suffer from various systematic uncertainty from interactions in nuclear, are dominated in $P_{tot} < 100 \text{ MeV}/c$. This region has much less background than the other. Thus, by separating P_{tot} into two bins, better sensitivity can be obtained. Estimated proton lifetime limits for $p \rightarrow e^+\pi^0$ and $p \rightarrow \mu^+\pi^0$ are 1.7×10^{34} years and 7.8×10^{33} years, respectively.

4. $p \rightarrow \nu K^+$

If a proton decays into ν and K^+ , momentum of K^+ is below Cherenkov threshold, and stops

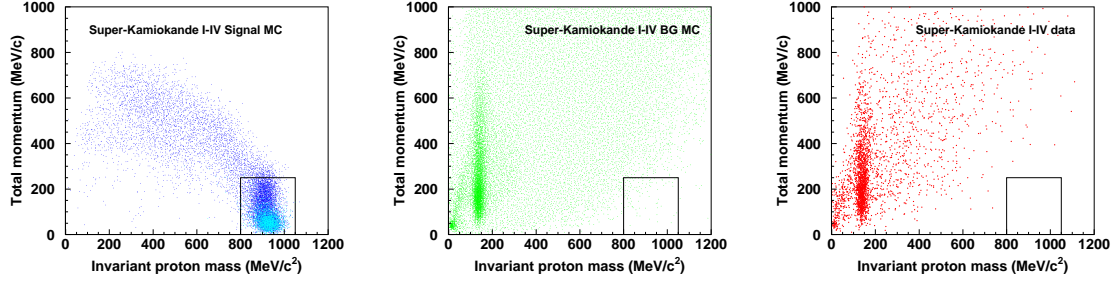


Figure 1: Reconstructed total invariant mass vs total momentum of signal MC (left), background MC (middle), and data (right) for $p \rightarrow e^+ \pi^0$ after all cut except (A-5) atmospheric ν MC. Light blue in the left figure shows free proton.

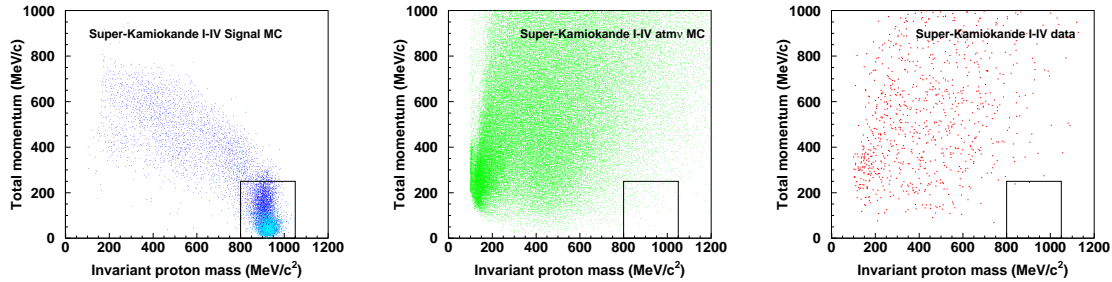


Figure 2: Reconstructed total invariant mass vs total momentum of signal MC (left), background MC (middle), and data (right) for $p \rightarrow \mu^+ \pi^0$ after all cut except (A-5) atmospheric ν MC. Light blue in the left figure shows free proton.

	$p \rightarrow e^+ \pi^0$			$p \rightarrow \mu^+ \pi^0$		
	Eff(%)	BKG(events)	Obs(events)	Eff(%)	BKG(events)	Obs(events)
SK-I	39.2	0.25	0	31.7	0.36	0
SK-II	38.5	0.12	0	31.3	0.15	0
SK-III	40.1	0.06	0	32.9	0.12	0
SK-IV	38.1	0.17	0	38.3	0.24	2

Table 2: Summary of efficiencies, expected numbers of background, and observed events in data. In SK-IV, Michael electron tagging efficiency has been improved due to new electronics and the efficiency for $p \rightarrow \mu^+ \pi^0$ is higher than the other periods.

in water and decays into $\mu^+ + \nu_\mu$ or $\pi^+ + \pi^0$ with monochromatic momentum in most of case. Thus, decay products from K^+ with 12 nsec lifetime are used for tagging this proton decay mode. In addition, after proton decay, gamma rays could be emitted due to deexcitation of the remaining nucleus, in which dominant energy is 6 MeV. This gamma ray acts as a prompt signal and the atmospheric ν background can be largely reduced if it is tagged. To detect $p \rightarrow \nu K^+$, three methods are applied; (B) tag muon with 236 MeV/c with prompt gamma ray, (C) fit μ momentum distribution of data with signal and background MC, (C) tag π^0 with 206 MeV/c.

For method (B), following cuts are applied to data and MC; (B-1) a fully contained event with one μ -like ring, (B-2) there is one Michel decay electron, (B-3) the reconstructed muon momentum is between 215 and 260 MeV/c, (B-4) the distance between the vertices of the muon and the Michel electron is less than 200 cm, (B-5) the TOF-subtracted timing distribution for the muon vertex is required to have a minimum goodness-of-fit (> 0.6), (B-6) the pattern of the single μ -like ring is more likely to be a muon than a proton: $L_{pr} - L_\mu < 0$, L_{pr} , L_μ are likelihood functions assuming a proton and a muon, (B-7) gamma hits are found: $8 < N_\gamma < 60$ for SK-I, III, and VI, $4 < N_\gamma < 30$ for SK-II (B-8) the time difference from the gamma tag to the kaon decay is consistent with the kaon lifetime: $t_\mu - t_\gamma < 75$ nsec, (B-9) there are no neutrons, only for SK-IV. A 12 nsec time window runs from muon tail to the past to find maximum hit cluster produced by prompt γ . Figure 3 show number of PMT hits in the window after all cuts except itself.

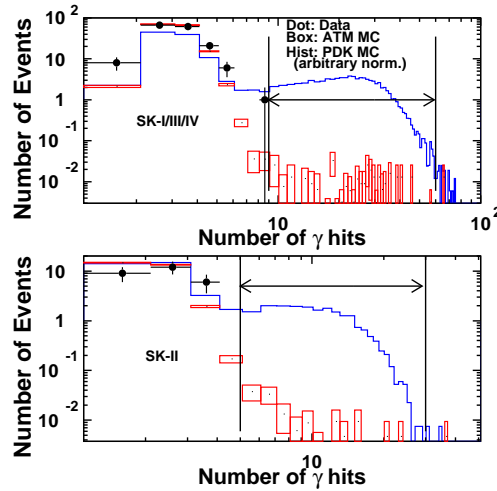


Figure 3: Number of γ ray hit distributions. The upper figure shows sum of SK-I, III, and IV which have 40% photo coverage, the lower figure corresponds to SK-II with 19% photo coverage. Bars, squares, and histogram correspond to data, atmospheric ν MC normalized to livetime of data, and proton decay MC with arbitrary normalization, respectively. The signal regions are indicated by arrows. The peaks at small numbers of hits are due to dark hits of the PMTs.

In method (C), rejected events by (B-7) are used to make μ momentum distribution to avoid duplicate data.

In method (D), stopped K^+ which decays into $\pi^+ + \pi^0$ is the target, but momentum of π^+ is close to Cherenkov threshold and it doesn't make clear ring. Thus we search for π^0 with 206 MeV/c

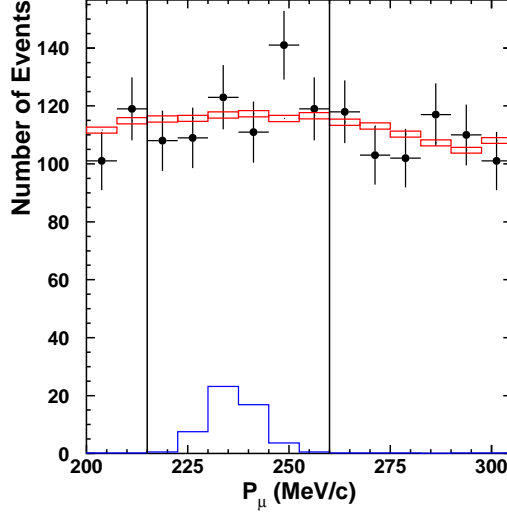


Figure 4: Muon momentum distribution for 260 kton-year. Dots, boxes, and histogram correspond to data, atmospheric ν MC, and proton decay MC, respectively. The data are fit by the background plus signal by free normalization. No excess above the expected background is observed. The normalization of the proton decay MC histogram shown is at the upper limit allowed by the fit.

in momentum, and PMT hit cluster in the backward of π^0 direction; (D-1) FC events with one or two rings and all rings are e -like, (D-2) one Michel decay electron from the muon produced by π^+ decay, (D-3) the reconstructed invariant mass of the π^0 candidate is between 85 and 185 MeV/ c^2 , (D-4) the reconstructed momentum of the π^0 candidate is between 175 and 250 MeV/ c , (D-5) the residual visible energy, defined as energy not associated with the π^0 nor the π^+ is low: $E_{res} < 12$ MeV for two-ring events and $E_{res} < 20$ MeV for single-ring events, (D-6) the likelihood for the photon distribution is consistent with that expected for signal events: $L_{shape} > 2.0$ for two-ring events and $L_{shape} > 3.0$ for single-ring events in SK-I/III/IV; $L_{shape} > 1.0$ for SK-II, (D-7) there is visible energy backwards from the π^0 direction consistent with a low momentum π^+ : $10 \text{ MeV} < E_{bk} < 50 \text{ MeV}$, (D-8) there are no neutrons, only for SK-IV. Detailed selection for $p \rightarrow \nu K^+$ can be found in Ref. [8]. Table 3 summarizes efficiencies, expected backgrounds, and observed events for method (B) and (D). No candidates have been observed for method (B) and (D) in 306 kton-years data. Selection efficiencies in SK-IV are higher than the other periods because the new electronics introduced in SK-IV contributes to increase Michel electron finding efficiency which is used in the selection in (B) and (D). Figure 4 shows momentum distribution for FCFV single ring sample in data, atmospheric ν MC, and signal MC. There are no excess in the signal region. Combining these three methods, the lifetime limit for $p \rightarrow \nu K^+$ is obtained as 6.6×10^{33} years.

5. SUMMARY

Super-Kamiokande has been search for nucleon decay but no evidences has been observed so far. In $p \rightarrow \mu^+ \pi^0$, two candidates are found but it is consistent with expected background. No

		SK-I	SK-II	SK-III	SK-IV
Exp.(kt-yrs)		91.7	49.2	31.9	87.3
Prompt γ	Eff.(%)	7.9	6.3	7.7	8.5
	BKG	0.08	0.14	0.03	0.14
	OBS	0	0	0	0
$\pi^+\pi^0$	Eff.(%)	7.8	6.7	7.9	9.0
	BKG	0.18	0.17	0.09	0.12
	OBS	0	0	0	0

Table 3: Summary of the proton decay search with selection efficiencies and expected backgrounds for each detector period.

candidates are observed for $p \rightarrow e^+\pi^0$ and $p \rightarrow \bar{\nu}K^+$. The lower proton lifetime limits are set to be 1.7×10^{34} years, 7.8×10^{33} years and 6.6×10^{33} years for $p \rightarrow e^+\pi^0$, $p \rightarrow \mu^+\pi^0$, and $p \rightarrow \bar{\nu}K^+$, respectively.

6. ACKNOWLEDGMENTS

We gratefully acknowledge the cooperation of the Kamioka Mining and Smelting Company. The Super-Kamiokande experiment has been built and operated from funding by the Japanese Ministry of Education, Culture, Sports, Science and Technology, the United States Department of Energy, and the U.S. National Science Foundation. Some of us have been supported by funds from the Korean Research Foundation (BK21), the National Research Foundation of Korea (NRF-20110024009), the State Committee for Scientific Research in Poland (grant1757/B/H03/2008/35), the European Union FP7 (DS laguna-lbno PN-284518 and ITN invisibles GA-2011-289442), the Japan Society for the Promotion of Science, and the National Natural Science Foundation of China under Grants No.10575056.

References

- [1] H. Georgi and S. L. Glashow, Phys. Rev. Lett. **32**, 438 (1974).
- [2] J. Wess and B. Zumino, Nucl. Phys. B **70**, 39 (1974).
- [3] W. J. Marciano and G. Senjanovic, Phys. Rev. D **25**, 3092 (1982).
- [4] N. Sakai and T. Yanagida, Nucl. Phys. B **197**, 533 (1982); S. Weinberg, Phys. Rev. D **26**, 287 (1982).
- [5] S. Fukuda *et al.*, Nucl. Inst. and Meth. A **501**, 418 (2003).
- [6] H. Kume *et al.*, Nucl. Inst. and Meth. **205**, 443 (1983); A. Suzuki *et al.*, Nucl. Inst. and Meth. A **329**, 299 (1993).
- [7] H. Nishino *et al.*, Nucl. Inst. and Meth. A **610**, 710 (2011); S. Yamada *et al.*, IEEE Trans. Nucl. Sci. **57**, 2010, 428.
- [8] The Super-Kamiokande Collaboration, Phys. Rev. bf D90, 072005 (2014).